Leontidis *et al. Geothermal Energy* (2025) 13:10
https://doi.org/10.1186/s40517-025-00331-y

Geothermal Energy

RESEARCH Open Access

Controlling injection conditions of a deep coaxial closed well heat exchanger to meet irregular heat demands: a field case study in Belgium (Mol)

Vlasios Leontidis[1*], Edgar Hernandez[2*], Justin Pogacnik[2], Magnus Wangen[3*] and Virginie Harcouët-Menou[2]

*Correspondence: vlasios.leontidis@ifpen.fr; edgar.hernandez@vito.be; magnus.wangen@ife.no

[1] IFP Energies Nouvelles, 1 & 4 Avenue de Bois Préau, 92852 Rueil-Malmaison, France
[2] Flemish Institute of Technological Research (VITO), Boeretang 200, 2400 Mol, Belgium
[3] Institute for Energy Technology, Instituttveien 18, Kjeller 2027, Viken, Norway

Abstract

Deep geothermal closed-loops have recently gained attention because of their advantages over classical geothermal applications (e.g., less dependence on the geology, no risk of induced seismicity) and technological advantages (e.g., in the drilling process, use of alternative to water fluids). This paper deals with the repurposing of an existing well in Mol, Belgium, by numerically evaluating the closed-loop concept. Two numerical tools are used to predict the evolution of the temperature and the produced energy over a period of 20 years considering the vertical coaxial well and the complete geological morphology. Full-scale simulations are initially carried out to estimate the maximum capacity of the well and to highlight the need to control the output of the well by adjusting the inlet conditions. Simulations are then performed either to deliver a constant power or to cover irregular thermal energy demands of two buildings by applying in both cases three process control operations. Through controlling the inlet temperature, the injected flow rate or successively both, the production of excess energy, resulting from the overdesign of the existing wellbore for the specific application, is limited. The simulations showed that continuous adjustments to the injection temperature and/or flow rate are needed to restrict the rapid drop in outlet temperature and consequent thermal depletion of the rocks, caused by the highly transient nature of the diffusive heat transfer from the rocks to the wellbore, as well as to supply a specific heat demand, constant or irregular, over the long term. In fact, the combination of both controls could be the ideal strategy for supplying the demand at the highest COP.

Keywords: Deep borehole heat exchanger, Closed-loop geothermal system, HOCLOOP, Numerical modelling, Heterogeneous formation, Irregular heat demand, Process control

Introduction

Open loop geothermal applications, using doublets or multiple injection and production wells, extract hot water from a geothermal reservoir, like an aquifer, and reinject cold water in the same reservoir. These applications initially rely on forced convective heat

transfer through the withdrawal of the in-situ hot water, and ultimately, on both diffusion and forced convective heat transfer processes, which are promoted by the injection of the cold water. In Europe, depending on the type of geothermal aquifer, the thermal energy output of these projects can reach the order of gigawatts (GW) for thermal power and hundreds of megawatts (MW) for electric power for high enthalpy reservoirs (Manzella et al. 2019; Ragnarsson et al. 2021; Melikoglu 2017). On the other hand, medium-to-low enthalpy geothermal doublets, like those developed in the Netherlands (Willems and Nick 2019) or in Paris basin (Lopez et al. 2010), can typically produce from 1 MW up to 20 MW of thermal energy. Despite their relatively high energy output, open well systems have several limitations primarily related to geological constraints:

- High enthalpy reservoirs are found in specific geological areas, which are limited worldwide.
- Due to rock heterogeneity and limitations of the exploration techniques, the risk of encountering a reservoir with poor petrophysical properties are high, especially when targeting underexplored and/or deep aquifers.
- The injection of cold water at excessive pressure next to or into faults could lead to fault reactivation (Kruszewski et al. 2023), induced seismicity (Buijze et al. 2019) and interference between multiple doublets (Daniilidis et al. 2021).
- Decrease or loss of injectivity with time (Luo et al. 2023).
- The produced fluid may carry unwanted impurities (toxic solvents and non-condensable gases) to the surface that should be treated as pollutants incurring disposal costs (Rose et al. 2020). Alternatively, they can be fully reinjected back to the reservoir (Leontidis et al. 2023).

Alternative conceptions of geothermal open-loop systems exist in literature, for instance, semi-open single-wells that are open-loop systems where the working fluid, water or supercritical CO_2, is recirculated inside the wellbore and allowed to flow into the surrounding rocks which can improve heat transfer (Hernandez Acevedo and Rodriguez Hernandez 2024). This is accomplished by leaving the well open (no casing) along continuous or locally permeable and non-permeable intervals. Flow interaction with the near wellbore rock is induced by placing flow restrictions (like a packer) in the well-tubing annular space that divert part of the working fluid into these intervals. The main challenges of this type of single well applications are complexity in the well completion, interaction between the working fluid and the formation fluid, plugging of the rocks due to sediments and scales deposition.

To overcome or mitigate the above-mentioned issues, new geothermal systems designs are emerging. Single deep closed-geothermal wells consist in the recirculation of a working fluid in a fully cased wellbore. The process is as follows: cold water (or any other carrier fluid, such as supercritical CO_2) is injected in the casing–tubing annular space, the temperature difference between the surrounding rock and the working fluid promotes the heat exchange via conduction. Once the fluid reaches the bottom of the well, it returns to the surface via a coaxial tubing. In contrast with shallow closed-loop single well systems, the applications of coaxial deep borehole heat exchangers are not common (Santos et al. 2022; Chen and Tomac 2023). These applications first appeared during the

1990s with both experimental (Morita et al. 1992) and commercial (Kohl et al. 2002) applications. The commercial experience in Weggis, Switzerland (Kohl et al. 2002) and the aborted attempt in Aachen, Germany (Dijkshoorn et al. 2013) highlight the need to design these closed-loop systems for covering fluctuating daily heat demands, which are common in residential and offices buildings. This requires changing the injection conditions (flow rate and injection temperature) in timeframes of months, days, or hours. Furthermore, the solution of closed-loops could be promoted by the repurposing of existing or abandoned wells (e.g., from oil and gas or geothermal applications) to significantly lower capital and levelized costs (Beckers et al. 2022).

Borehole heat exchangers and geothermal doublets (with heat pumps) were recently compared for intermediate depths (< 2 km) at a cold sedimentary basin in Canada (Gascuel et al. 2024). It was shown that under the optimal flowing conditions for each system the sub-horizontal well doublet could produce far more energy when compared to a closed well. The optimal flow corresponded to either the flow rate that allows the maximum net energy production for the closed system or the maximum flow rate that allows the injection pressure to remain safe for the doublets. However, considering the particularities of the location (limited permeability), the heating power from the open systems dropped by one order of magnitude and became comparable with the closed-loop. Furthermore, the installation of a borehole heat exchanger would be safer, because of clogging and corrosion issues that are possible in the area.

The use of working fluid different than water, such as CO_2 (Hu et al. 2020b), ammonia (Chen et al. 2022) and other low boiling point fluids, is a current topic of research in the case of closed wells. The performance of these applications may be improved because they benefit from phenomena that are not encountered or are limited with water. For example, due to the large difference in fluid's density, caused by the temperature change along the downward and the upward sections, the fluid may circulate without a pump (thermosyphon effect) (Amaya et al. 2020). On the other hand, the heat transfer between the rock and the alternative working fluids can take place under two-phase thermodynamic state. This results in an almost constant temperature in the wellbore, which maximizes the temperature difference between the fluid and the rock, thereby enhancing heat flow. These fluids have been successfully tested at field scale (Chen et al. 2024).

The HOCLOOP project ("A circular by design environmentally friendly geothermal energy solution based on a HOrizontal Closed LOOP") aims to verify a novel geothermal closed-loop solution for the extraction of heat from deep or shallow formation rocks. The solution is based on new deep well construction technology for installing the insulated production string (Vestavik et al. 2017). The project develops the tools to enable the innovative geothermal solution and will demonstrate the technology in a full-scale test operation in Stavanger, Norway. The project covers the development and validation of numerical models for the heat flow and investigates the possibility for improving the electricity production by using alternative to water fluids. It also covers the investigation of potential EU pilot sites, environmental assessment, and the social acceptance (in Belgium, France, Italy, Germany and Poland).

One of the practical problems that faces the HOCLOOP solution, as well as other closed-loop and open-loop well applications, is the definition of the well operational conditions (flow rate and/or injection temperature) that could satisfy irregular heat

demand profiles. This is because the diffusive heat flow from the rock to the well is a highly transient phenomenon depending mainly on the residence time of the fluid in the well (Alimonti et al. 2018) and rock thermal conductivity. Both the wellbore heat transfer and the overall heat production depend on the inlet conditions, i.e. on the flow rate and to a smaller extend on the inlet temperature of the fluid, for a specific well configuration (Song et al. 2018). Thus, a certain well flow rate that can satisfy today's energy demand might not be sufficient to satisfy this demand in the future, and it might need to be increased at the expenses of lower production temperature but for the same amount of produced heat. Such prediction requires numerical tools that are accurate and computational efficient to handle the time-dependent process control.

These irregular heat demand profiles are common in real applications. Thus, a control method is required for providing the required heat that also considers the transient nature of the heat flow from the rock towards the well. There are two operational conditions that can be controlled for adjusting the output energy to meet a varying demand: fluid rate and injection temperature. For instance, one approach, which is a good option for periods where the variation in heat demand is relatively small, is keeping fluid rate constant and varying the injection temperature in accordance with the energy demand. The second option, which is an alternative for covering large changes in heat demand like those occurring during seasons and months, is changing the fluid rate while keeping relative constant the injection temperature. The combination of these two approaches was applied in Weggis deep closed-loop single well project (Kohl et al. 2002).

Through numerical simulations, it was shown that a deep borehole heat exchanger (around 2000 m) for a low-temperature geothermal fluid (35–40 °C) running under constant flow rate (6 kg/s) can cover part (< 69%) of the heat demands of a 4600 m^2 offices building (Huchtemann and Müller 2014). A start and stop process with different ratios (durations of each interval) have been numerically tested to evaluate the impact on the outlet temperature and the heat production (Wang et al. 2022; huajun et al. 2022) or to find the optimal ratio for better heat extraction over a 20-year period (Guo et al. 2024).

For closed-loop systems detailed numerical simulations can be found in the literature that address the impact of different geological parameters, mainly the thermal conductivity and the geothermal gradient, in their performance (Kolo et al. 2024). Generally, a borehole heat exchanger should target locations with high rock conductivity and high temperatures. The first parameter facilitates the heat transfer due to conduction, while the second increases the available for recovery thermal energy.

This paper introduces two numerical tools that are coupled with a control scheme for adjusting well flow rate and inlet temperature to fulfil energy demands. The tools are validated against analytical solutions and commercial software and the control schemes are tested against constant and irregular heat profiles. For numerically testing the concept, geological and heat demand information from a potential HOCLOOP testing site, located in Belgium (Bos and Ben 2017), are used. For the specific site the properties of the geological setting (thermal conductivity, heat capacity, geothermal gradient) are well documented.

Methods

Case study

The VITO open-loop geothermal project, located in Mol, Belgium, has been chosen as a reference case due to the detailed geological and well information available (Bos and Ben 2017). The purpose of this project is the extraction of hot water (120–130 °C) for heating the facilities of the Flemish Institute of Technological Research (VITO) and to serve as a research playground for testing new geothermal technologies and proving geological concepts. The faulted and fractured limestones from the lower Carboniferous host the aquifer under production in this project (Fig. 1). Three wells were drilled through this aquifer, reaching depths between 3000 to 4230 m. One of these wells, MOL-GT-03, did not find sufficient permeability in the aquifer for either injection or production,

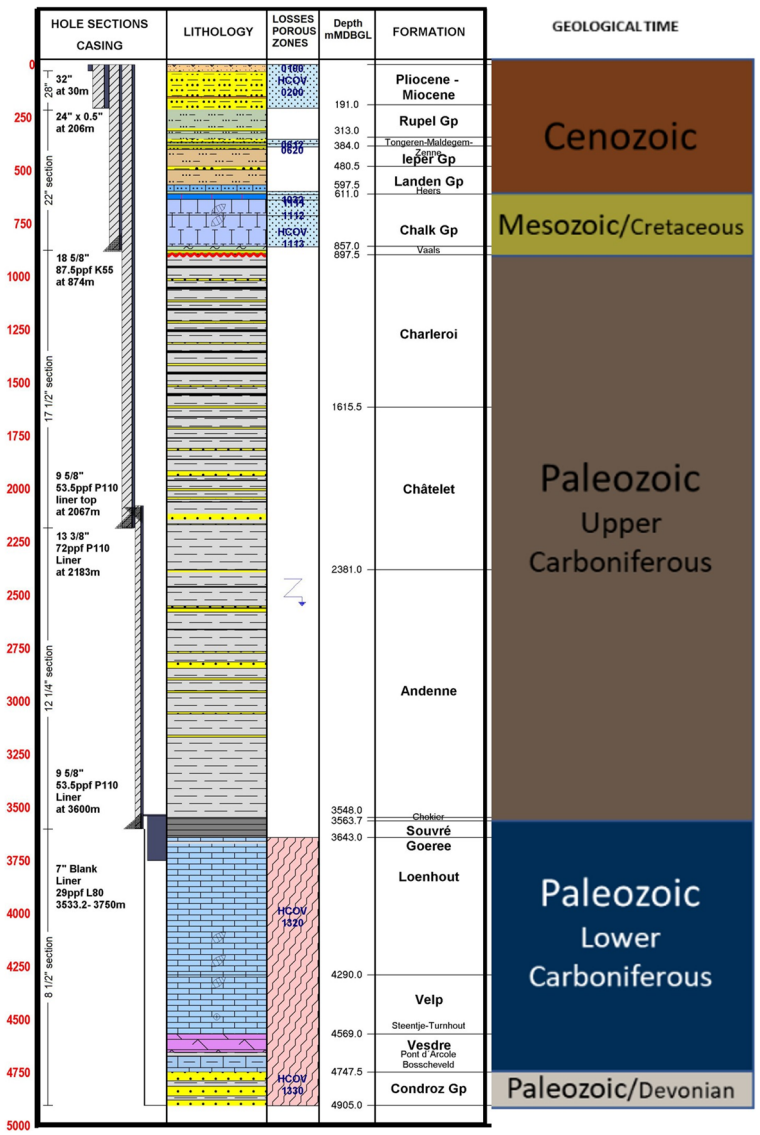

Fig. 1 Description of MOL-GT-03 cased and non-cased sections and drilled geological formations with its corresponding geological time (copyright VITO)

becoming a candidate for drilling a side-track, for abandonment or for testing new technologies. The latter option is considered in this paper for evaluating the closed-loop concept in its current state and under the HOCLOOP concept, which implies the use of the envisaged insulated production string. In this evaluation, the entire well trajectory is considered.

Well and rock characteristics

The chosen well is inclined, with a total trajectory of 4905 m and a total vertical depth of 4230 m. It is cased until a depth of 3750 m and passes through sedimentary rocks of different ages and lithologies as shown in Fig. 1. This causes thermal rock properties and consequently temperature gradient to change along the well trajectory as indicated in Table 10 (all necessary data to reproduce the results are included in the Appendix). The casing system comprised multiple layers of cement and steal casing (tubular sections). The dimensions and properties of these layers are indicated in Table 11, with the characteristics of the insulated tubing developed for the HOCLOOP concept in Table 12.

Site potential

Initially, the potential of the site is investigated by performing full-scale simulations considering the detailed properties of the wellbore and the rocks. Three flow rates (3, 5 and 7 kg/s) and two inlet temperatures (20 °C and 40 °C) are tested for a period of 20 years. During the simulations all other parameters are kept constant and the evolution with time of the outlet temperature and produced energy is traced. Due to the deep depth of the well and the high geothermal temperature, the borehole heat exchanger is expected to be able to produce sufficient thermal energy to cover potential demands.

Energy demand

Nearby the well location, two new office buildings are under construction. The heating system of these buildings has been conceived for low-temperature input water (minimum 45 °C) and output temperature (40 °C). A typical 12-hourly evolution of the heat demand for one year is given in Fig. 2.

Two scenarios of energy demand are considered for the Belgian reference case that are also used for testing the operation control schemes:

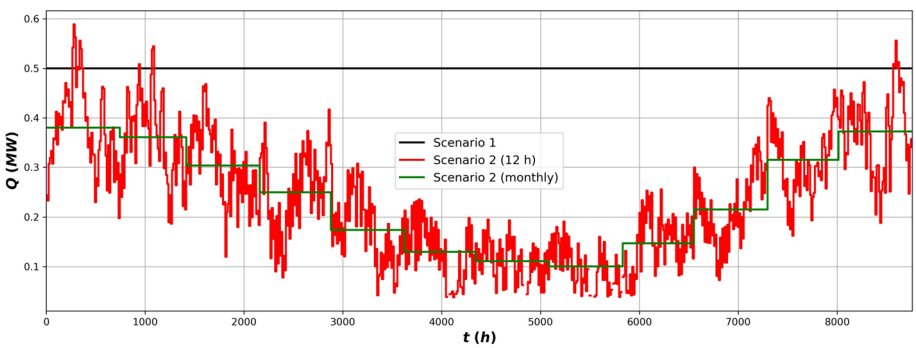

Fig. 2 12-h estimated heat demand and monthly averages for the reference case for one year

Table 1 Controlling processes for constant delivered power (Scenario1, 0.5 MW)

Control system	Controlled parameter	m_{init} (kg/s)	m_{init} (kg/s)	T_{inj} (°C)
1	Inlet temperature	2–12	N/A	Calculated
2	Flow rate	Calculated	N/A	40
3	Dual	2	N/A	Calculated
3	Dual	5	0.5	Calculated

Table 2 Controlling processes for irregular demands (Scenario 2)

Control system	Controlled parameter	m_{init} (kg/s)	Δm (kg/s)	T_{inj} (°C)
1	Inlet temperature	2, 3	N/A	Calculated
2	Flow rate	Calculated	N/A	40
3	Dual	1.5	0.5, 1	Calculated

1. Constant thermal power demand of 0.5 MW (or 4.4 GWh/y) for 20 years (Scenario 1). This demand corresponds to a value close to the maximum (peaks) demand of the case study shown in Fig. 2.
2. Seasonal energy demand (around 2 MWh/y) for 20 years (Scenario 2) with a monthly demand (according to Fig. 2). In addition, a seasonal case is run, considering a 12-h demand to evaluate the impact of peaks (maximum and zero demands).

Control process

Excess heat generation can occur when the flow rate and/or produced fluid temperature are sufficiently high, causing the delivered energy to exceed the demanded, leading to excess cooling and energy waste. To avoid power overproduction, solutions include limiting the system installation to a specific section of the existing well or adjusting flow conditions in the primary (well) or/and the secondary (heat exchanger) systems. For this study, the approach chosen is to utilize the actual full length of the well and adjust the inlet fluid conditions to align the heat production with the demand.

Description of the control systems simulations

The options for controlling the well flowing conditions and meet demand are:

Control 1: Adjust the inlet (injection) temperature for a fixed flow rate.
Control 2: Adjust the injection flow rate while keeping constant injection temperature.
Control 3: Dual control of the system where both injection temperature and flow rate are adjusted in sequence. The control process is started with Control 1 followed by Control 2 when minimum injection temperature is reached.

The two energy demand profiles mentioned previously are considered as the main simulation scenarios. The first scenario evaluated is a constant demand profile (0.5 MW) over 20 years. The different control systems, detailed in Tables 1 and 2, are tested with

two temperature restrictions, which are imposed from the design of the heating system in the buildings:

1. The minimum inlet temperature is set at 40 °C.
2. The minimum outlet temperature is 45 °C.

For Control 1, the initial flow rate is constant throughout the simulations and the injection temperature is continuously calculated, and vice versa for Control 2. For Control 3 an initial flow rate is set, and the model calculates the injection temperature. Afterwards, it either calculates the flow rate or sets a gradual increase of the flow rate (Δm) whenever the temperature is about to fall below 40 °C (Table 1). For Control 1, several flow rates are tested to define the optimal operational point, whereas for Control 2 only one operation point exists considering the nominal injection temperature. In Control 3, two initial flow rates cases are tested, a low value and with a continuously updated flow rate and a higher value with a stepwise increase.

The second demand scenario, which corresponds to a more irregular heat demand, is tested with the three mentioned controls to show how temperature and flow rates may vary in a more practical problem. For Control 1, two flow rates are tested, and for Control 3 an initial flow rate but with two gradual increases. Like Scenario 1, one case is tested for Control 2 (Table 2).

Performance evaluation

For the long-term evaluation of the heating system, the heat extraction performance of the deep geothermal closed well and the power consumption of the circulation pump are considered via the COP (coefficient of performance), which is defined here as the ratio of the produced (delivered) heat, E_{prod}, to the energy losses, E_{losses}, according to Eq. (1) (Lund 2024). The latter consists of the energy spent to pump the fluid in the closed well, W_{pump}, and the mismatched energy between the demanded, E_{ref}, and the energy delivered by the system. Thus, what is not covered by geothermal must be covered by an external source.

$$\text{COP} = \frac{E_{\text{prod}}}{W_{\text{pump}} + \left|E_{\text{ref}} - E_{\text{prod}}\right|} \tag{1}$$

The produced energy can be calculated by the integration of the temporal evolution of the produced heat, Q [w], while the pumping energy by the integration of the temporal evolution of the pressure losses, ΔP [Pa] (pressure difference between outlet and inlet), as:

$$E_{\text{prod}} = \int Q dt \tag{2}$$

$$W_{\text{pump}} = \int \frac{m \Delta P}{\rho \eta} dt \tag{3}$$

where m [kg/s] is the mass flow rate, ρ [kg/m^3] is the density of the fluid, η is the efficiency of the pump (0.85 in the study) and dt the duration of integration interval. Simpson's rule is applied to estimate the integrals of Eqs. (2) and (3) either for each year or for the whole duration of the calculations (cumulative COP).

Here only the borehole heat exchanger is considered, and the results are used to compare the different scenarios of operation without considering a heat pump or a secondary heat exchanger for recovering the heat for the buildings and reinjecting the fluid in the desired temperature.

Tools

GTW and GWellFM simulators

Two in-house numerical simulators are used in the study: GTW from IFE and GWellFM from IFPEN. Both tools:

- are 1D and axisymmetric;
- are semi-transient geothermal simulators in cylinder coordinates solving the equation for transient heat conduction for cooling or heating of the rock, assuming, however, stationary advective (by the fluid) and convective heat transport in the wellbore;
- solve the momentum, energy and mass balances;
- calculate the heat losses due to conduction and forced convection, as well as pressure losses due to friction and gravity in both legs of the wellbore.

GTW (geo-thermal-well) is a single-phase and semi-transient geothermal simulator in cylinder coordinates (Wangen 2024). The simulator obtains the numerical solution using an energy-conservative finite volume method. The energy transfer across cell boundaries is energy conservative in both the rock and the well. Local energy conservation for each cell implies global energy conservation for the combined system of well and rock.

GWellFM (geothermal well flow model) considers the single-phase flows of liquids and gases, the hydrodynamics of the two-phase downward and upward flows, constitutive laws for mixtures, and the heat exchange between the well completion and the surrounding formation (Leontidis et al. 2023). The model is fully compositional and, to perform thermodynamic calculations, a thermodynamic engine has been integrated into the code (Hemptinne et al. 2023). Calculations are performed in thermodynamic equilibrium and several equation-of-states are available (i.e. Cubic-Plus-Association, Peng–Robinson, GERG-2008, Kestin) (see Table 3).

Boundary conditions and computational parameters

In all simulations, a constant temperature is imposed in the surface cell (Dirichlet boundary condition), whereas a Neumann boundary condition of null heat transfer is imposed in the lateral border (Fig. 3). The bottom border in GWellFM is located at the end of the wellbore applying a Neumann boundary condition, while in GTW the border is placed 100 m deeper from the completion applying a Dirichlet boundary condition. For deep boreholes and closed wells, the impact of the different boundary conditions in the bottom border is limited and restricted in the regions close to the border, because

Table 3 Summary of cases by simulator

Type of simulation	Tool
Benchmarking	Both
Full-scale	GWellFM
Scenario 1, Control 1	GWellFM
Scenario 1, Control 2	GTW
Scenario 1, Control 3	GWellFM
Scenario 2, Control 1	GTW
Scenario 1, Control 2	GTW
Scenario 2, Control 2	GWellFM

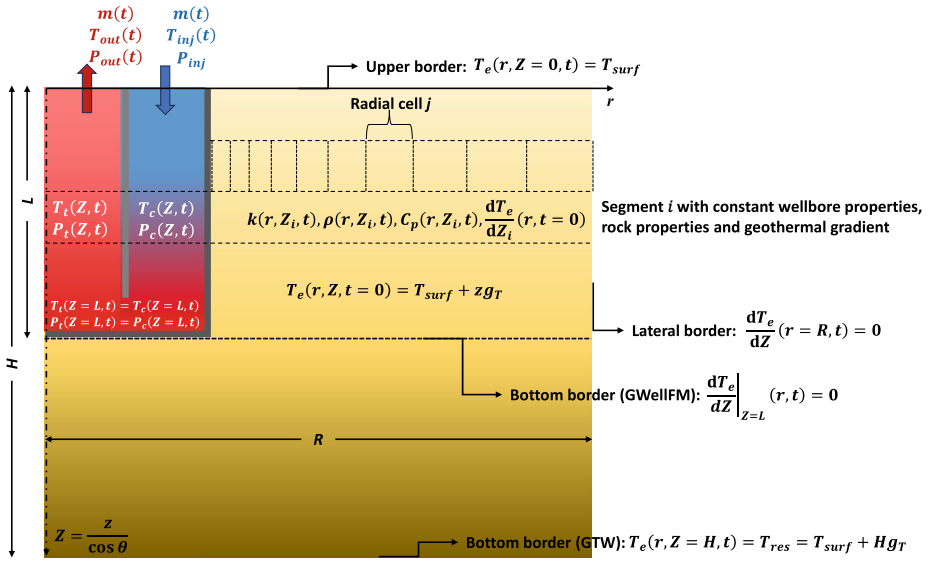

Fig. 3 Schematic representation of the computational domain and the numerical settings

the axial heat transfer rate is quite low especially when compared to the radial heat transfer rate.

The domain is initialized with the geothermal gradient, and the mass flow rate, temperature and pressure of the fluid in the inlet of the annulus compartment are set as initial values. At the bottom of well, the pressures and the temperatures in the annulus (casing side) and the central tubing are always equal.

A minimum and a maximum adaptive time step of 6 h and 2 weeks is used in GWellFM and 0.01 h and 12 weeks in GTW, respectively. In both tools, the time step is initialized to the initial step with every modification in the inlet conditions.

The computational domain is discretized in the axial and radial direction, using a linear and a geometric mesh, respectively. In the axial direction, the grid is always vertical, and it is modified to account for the inclination of the wellbore. In this way, all calculations are done along the measured depth (MD) of the wellbore and not along the true vertical depth (TVD). The axial discretization of the wellbore is done per segment, with each segment having constant properties (wall layers, type of rocks and geothermal gradient) and meshed with around 15 m length cells (329 cells in total). The radial mesh

is refined close to the well, where the changes in the temperature are expected to be sharper. The radial size of the domain is always 100 m with 50 cells with a minimum cell size of 1 mm for GWellFM and 25 cells for GTW.

It should be noted that the considered central tubing consists of three coaxial layers: an inner steel tube, an insulation layer, and an outer tube. However, due to the limitations of the GTW code in the number of the wall layers that can be considered, an overall diameter and an average thermal conductivity are used. The space between the two tubes is in vacuum with an estimated thermal conductivity of 0.01 W/m/K. Furthermore, both in the inner tube and the casing a roughness of 0.15 mm is considered to account for the losses due to friction in the walls.

The numerical tools could either use pressure–temperature dependant fluid properties (density, thermal conductivity, heat capacity) or pre-defined constant values. In the results presented hereafter the fluid properties are constant (see Appendix) for the benchmarking (Sect. Benchmarking) and two thermal energy demand scenarios (Sect. Energy demand: Scenario 1), while in the full-scale simulations (Sect. Site potential) the properties are updated at every cell with the local pressure and temperature. In the Discussion Sect. (Impact of fluid properties), the impact of between the two cases is investigated.

Solution for the process control systems

Optimization routines were developed to properly define the well flow rates or injection temperatures. The optimization process is an iterative procedure based on Broyden's method, a quasi-Newton method for finding roots. It is used as an alternative to Newton's method due to its simplicity and its lower computational cost. The power and temperature delivery are evaluated at the end of every optimization (GTW) or every simulation time step (GWellFM) to determine if the well can meet the exact required power/temperature, without excess.

For flow control in GTW, if output power is above or below the demand, flow rate is decreased or increased, respectively, via Broyden's method during every optimization time step; and if temperature is equal to the minimum input temperature of the building's heat exchanger, flow rate is decreased and less power than the required is delivered. Thus, the minimum required delivery temperature is given priority. An initial guess at the required flow rate is made based on the flow from the previous production period. The flow is changed until a convergence in power of 10^{-5} W is reached. In practice, flow steps typically converged in less than 7 iterations with this procedure. The restart option implemented in GTW simulator is leveraged to speed up computing time of every iteration.

Similar processes are implemented for the temperature control or the dual control in GWellFM. Nevertheless, the inlet temperature or the flow rate is optimized at every time step applying Broyden's method with a convergence criterion of 10^{-6}. If the inlet temperature is equal to the minima, the updated heat to be delivered is initially estimated from the flow rate and the temperature difference between well outlet and inlet. Control 3 is a combination of the two other control systems. Starts with Control 1 and once the minimum injection temperature is reached the system switches to Control 2. An initial constant flow rate is necessary to be set, according to process of

Control 1. The following table summarizes the simulations that are performed, and which tool is used for each case.

Results

Benchmarking

To benchmark the two in-house simulation tools, a case that has analytical solution for predicting fluid's temperature, is defined, and simulated. It is a vertical well with a coaxial returning pipe (Fig. 4) in a homogeneous formation (Table 13). Water with properties independent from pressure and temperature is injected by the annular space and the same fluid is recovered at the surface from the central tubing.

Ramey (1962) presented an analytical model to predict the heat loss between wellbore and formation in injection wells using a time function to describe the diffusion of heat from the outer wellbore radius to the infinite formation boundary. In case of coaxial wells, the Ramey solution could be applied only for the annulus fluid considering the heat exchange with the formation but not the heat interaction between the two fluids. Al Saedi et al. (2018) presented an analytical model for the wellbore fluid temperature for a drilling circulation system in a vertical well, both in the central tubing and the annulus as a function of the well depth and the time. All analytical solutions cannot directly consider lithologies and/or geothermal gradients that change with depth.

In addition to the analytical solutions, two commercial software are used to compare the results with the numerical tools:

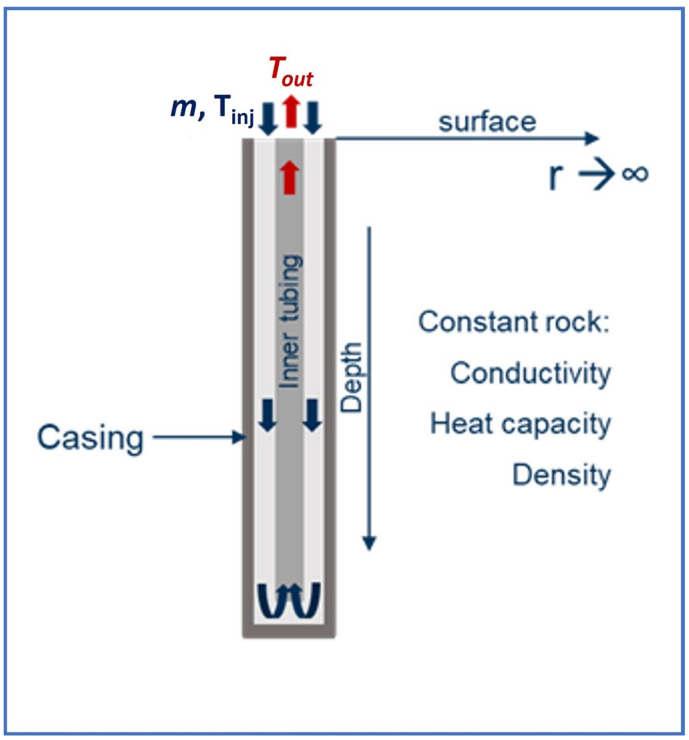

Fig. 4 Schematic representation of the benchmarking case

1. COMSOL Multiphysics® (Hu et al. 2020a; Wang et al. 2021) is used by discretizing the wellbore together with the rock system, such as the problem is solved fully coupled using steady-state flow in the well and transient 3D diffusive heat transfer in porous media.
2. The quasi-stationary method based on the analytical solution of Eskilson and Claesson available in FEFLOW® is also applied (Abesser et al. 2023; Le Lous et al. 2015). This option is suitable for long-term simulations with less frequent and less steep inflow temperature changes and provides a reasonable accuracy at lower computational cost.

Figure 5 depicts the temperature profile in the annulus (continuous line) and in the coaxial tubing (dashed line) at two times. The results of GWellFM and GTW are very close to the results of COMSOL and FEFLOW, whereas almost overlapped with the results of the analytical solution of Al Saedi. Main difference between the COMSOL model and the tested codes is the meshing strategy. 3D polar meshing of the wellbore (including the inner pipe) and the rock domain is used in COMSOL, while in GWellFM and GWT 2D the mesh consists of radial elements. On the other hand, FEFLOW seems to perform better at the long-term with the temperature profile approaching the analytical and numerical solutions. Finally, the analytical solution of Ramey can also predict the temperature in the annulus because the heat losses from the annulus towards the central tubing are limited. The inner tube is well insulated and the temperature difference between the two compartments is low. The maximum error in the calculations of the numerical tools when compared with the analytical solution of Al Saedi, expressed as the ratio of the differences between the numerical and the analytical results to the analytical results, is less than 0.3%.

Site potential

The full-scale simulations of the site are done with GWellFM, and the thermodynamic tool activated to consider the effect of pressure and temperature in fluid's properties. Figure 6 shows the evolution of the temperature and the pressure difference with the inlet pressure of the fluid both in the space between the casing and the central tubing and in the central tubing. While the fluid travels downstream in the annulus, it recovers energy from the rocks and its temperature increases. On the way up to the surface, the heat losses are limited because of the well-insulated central tubing and the

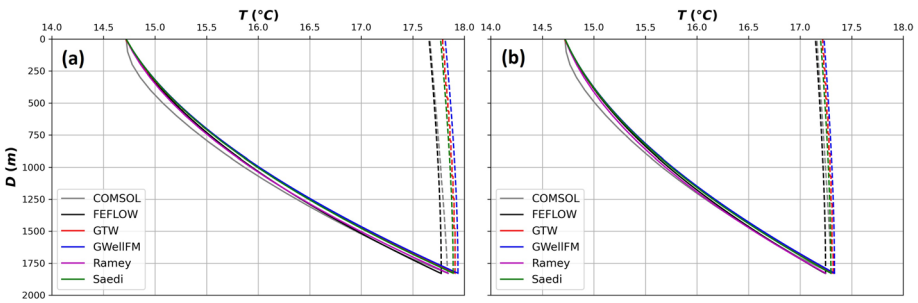

Fig. 5 Benchmarking results after **a** 1 year and **b** 10 years (solid lines: descending flow in the annulus, dashed lines: ascending flow in the tubing)

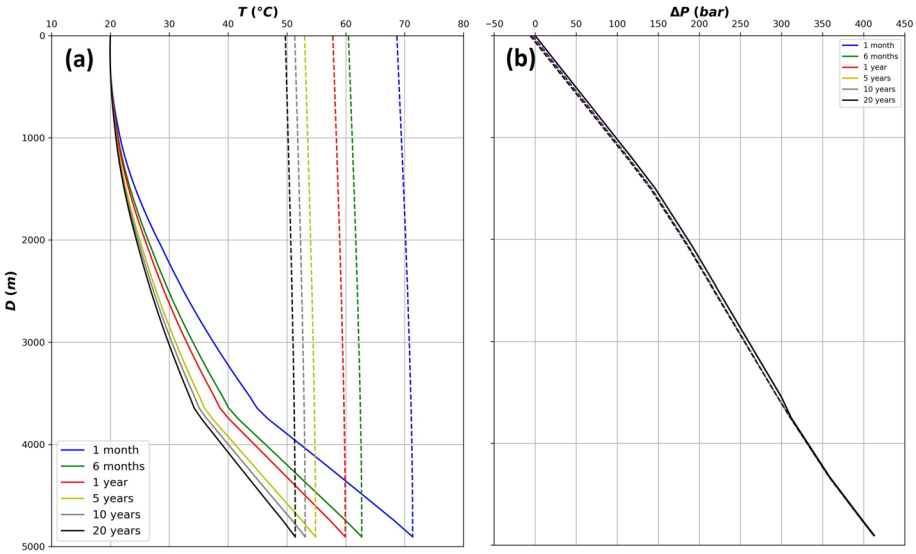

Fig. 6 Evolution of fluid's **a** temperature and **b** pressure difference in the annular space (solid lines) and the central tubing (dashed lines) for different times ($m = 5$ kg/s, $T_{inj} = 20$ °C)

temperature remains practically constant. The temperature of the fluid reduces with time as the surrounding wellbore rocks become colder.

Similarly, the pressure of the fluid increases with the depth in the annular space and decreases in the return tubing because of the gravity. On the other hand, the pressure of the fluid remains almost constant in time since the impact of the temporal evolution of the temperature through the physical properties is negligible. It should be noted that the fluid pressure at the wellhead level in the central tubing is slightly lower than the inlet pressure (negative pressure difference). This observation will be discussed in Sect. Impact of inlet conditions.

The output temperature and the gross thermal power potential of the selected well, estimated as the difference of the specific enthalpies between outlet and inlet multiplied by the flow rate, are shown in Fig. 7 as a function of flow rate and injection temperature over time. Thermal power output (Fig. 7b) is transient, reaching values close to 0.5 MW after 20 years. It is clearly seen that a constant flow rate and a constant injection temperature in the well cannot provide a constant power over time. Thus, a control on these conditions is needed to fulfil a specific demand.

This figure also shows that a higher flow rate, which means higher fluid velocity, results in lower residence time of the fluid in the well but higher heat transfer coefficient and higher temperature difference between the fluid and the rock. Thus, more heat is recovered from the hot rocks at the expense of lower outlet temperature. On the contrary, a higher injection temperature gives lower thermal power but higher output temperature when flow rate is kept constant. This is due to higher energy losses at shallow depths, where the temperature in the well is higher that the surrounding rock temperature, and the lower heat flows at intermediate and deep depths where fluid temperature is higher. This behaviour indicates that changing control conditions leads to changes in the output temperature and thermal power which sets the basis for the studied control schemes.

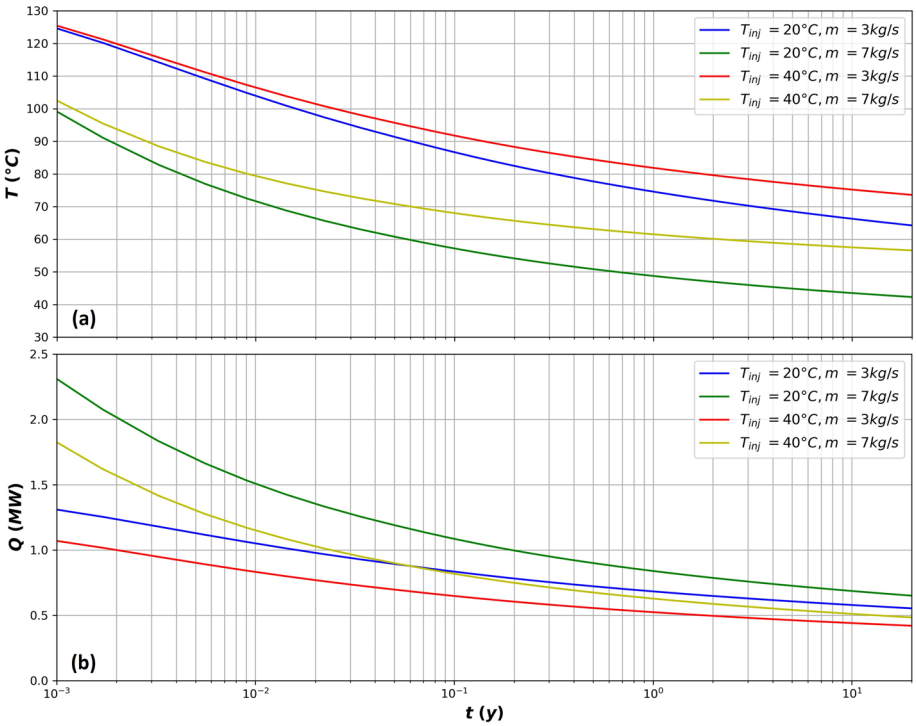

Fig. 7 Impact of wellhead temperature and flow rate on the outlet a temperature and b gross thermal power (time axis in logarithmic scale)

Table 4 Total produced gross thermal power over the 20-year period

m (kg/s)	T_{inj} (°C)	E_{tot} (GWh)
3	20	104.1
5	20	117.9
7	20	124.3
3	40	79.3
7	40	92.6

The total produced thermal power, which corresponds to the area below the curves, is given in Table 4. The higher the flow rate (or the lower the inlet temperature), the greater the power is produced.

Energy demand: scenario 1

Control 1: adjusting injection temperature

Figure 8 presents the evolution with time of the inlet and outlet temperature of the well for Control 1 and for the system to deliver 0.5 MW of energy. For low flow rates, the temperature differences between outlet and inlet are required to be sufficiently high to deliver the demanded power. Thus, the rates of energy recovery from the formation are higher and the decrease of temperature occurs with high gradients. As a result, the inlet temperature quickly reaches the minimum threshold of 40 °C. Increasing the flow rate reduces the rate at which the temperature decreases and delays the

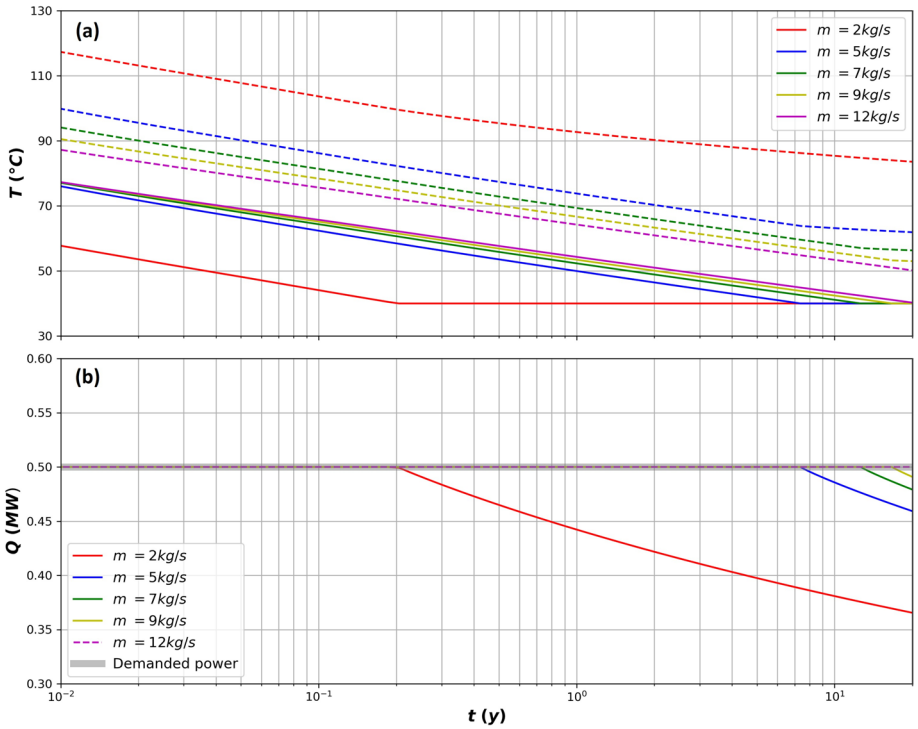

Fig. 8 Temporal evolution of a fluid temperature (solid lines: inlet; dashed lines: outlet) and b gross thermal power production for different flow rates for Scenario 1 (constant thermal power) and Control 1 (adjust of injection temperature)

power cut-off. There is a flow rate (around 12 kg/s) for which the system produces the demanded power for the simulated period. However, the flow rate increase is always accompanied with an increase in the pumping power, due to the friction losses.

The evaluation of the controlling system with different fixed flow rates is done by calculating and comparing the cumulative COPs over 20 years. Figure 9a shows that the COP depends strongly on the flow rate and there is an optimal flow rate for which COP reaches a maximum value. After this limit, the consumption of the injection pump starts to become very important when compared to the total produced energy. For the optimal flow rate (7 kg/s), the system covers 99% of the total demanded energy over the period of the 20 years.

Control 2: adjusting injection flow rate

For Control 2, the system can deliver continuously the demanded heat (Fig. 10) by increasing the flow rate without reaching the limit of minimum input temperature of the building's heat exchangers (minimum delivery temperature). The fluctuations observed in the power profile (peaks mostly present at early times) are because of the numerical procedure applied with GTW to solve the problem of controlling the flow rate. The procedure aimed to cover the heat demand at the end of the optimization time step while flow rate is kept constant which leads to these peaks or excess in power production.

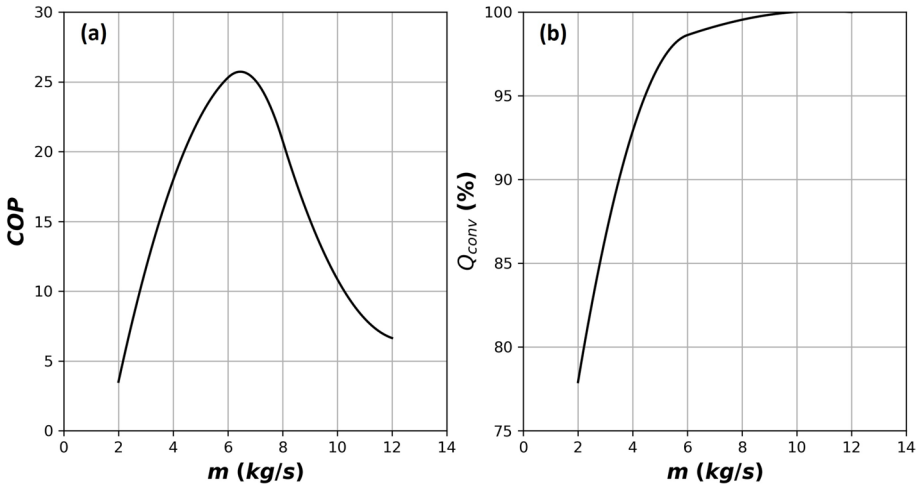

Fig. 9 **a** Cumulative COP and **b** demand covered for Scenario 1 (constant thermal power) and Control 1 (adjust of injection temperature) under different fixed flow rates

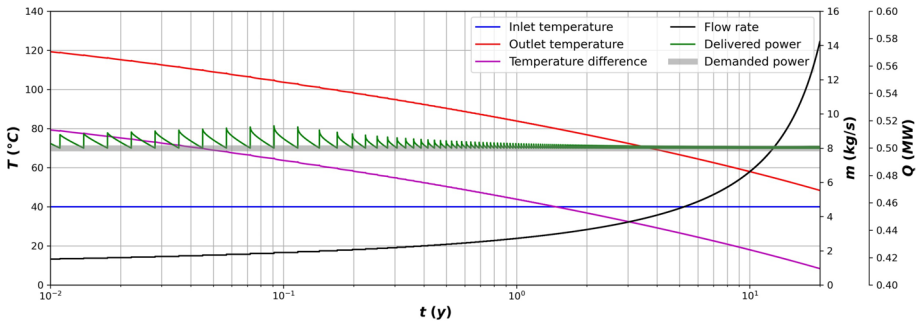

Fig. 10 Evolution of outlet temperature, gross thermal power and flow rate for Scenario 1 (constant thermal power) and Control 2 (adjust of flow rate)

Control 3: dual control system

With Control 3 (Fig. 11), the borehole heat exchanger can continuously produce the needed power by first reducing the inlet temperature, down to the threshold, with a constant flow rate (2 or 5 kg/sec) and then by increasing the flow rate for constant injection temperature (40 °C). The initial interval, during which the system works under constant flow rate, depends on the initial selected flow rate and it can be extended by setting a higher flow rate, accordingly to the results of Control 1, at the cost, however, of greater power consumption by the pump. For higher initial flow rate, the initial outlet temperature is lower, and the necessary inlet temperature is higher since lower temperature difference is needed to cover the demand.

Similar to Control 1, the COP is calculated for the two above systems with the results presented in Table 5. The performance of the system declines with the initial flow rate because the consumption of the pump is higher since higher flow rate is required for longer time.

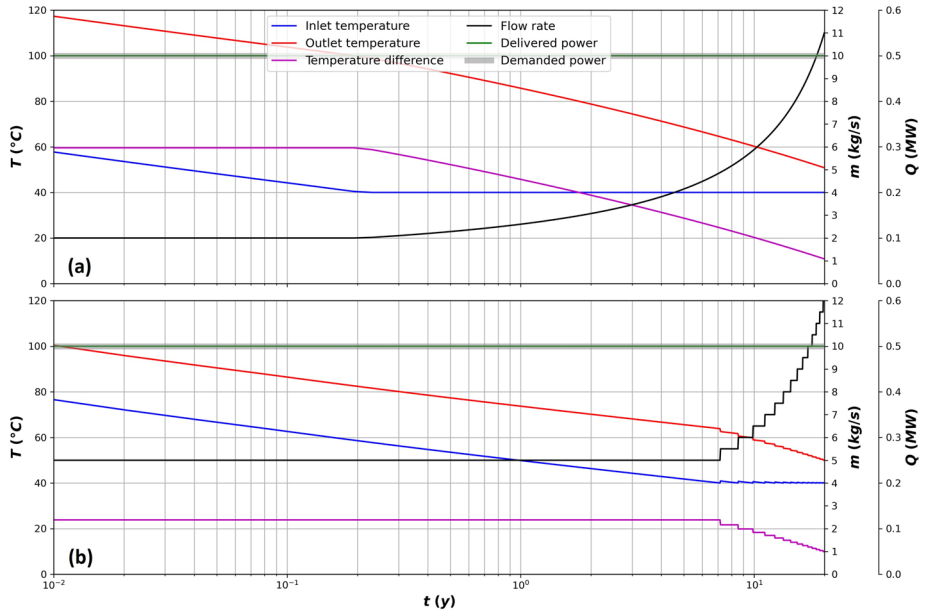

Fig. 11 Evolution of temperatures, gross thermal power and flow rate for Scenario 1 (constant thermal power) and Control 3 (dual adjustment) with a low initial flow rate and continuously updated flow rate increase and b higher initial flow rate and stepwise increase of the flow rate

Table 5 COPs for Control 3 (dual adjustment) and Scenario 1 (constant thermal power)

m_{init} (kg/s)	m_{max} (kg/s)	ΔP (bar)	T_{inj} (°C)	T_{prod} (°C)	W_{pump} (GWh)	COP (cumulative)	COP (@ 20th year)
2	11.0	< 45.0	< 72.4	> 80.8	2.64	9.4	33.1
5	12.0	< 52.5	< 92.6	> 50.0	3.41	7.4	25.6

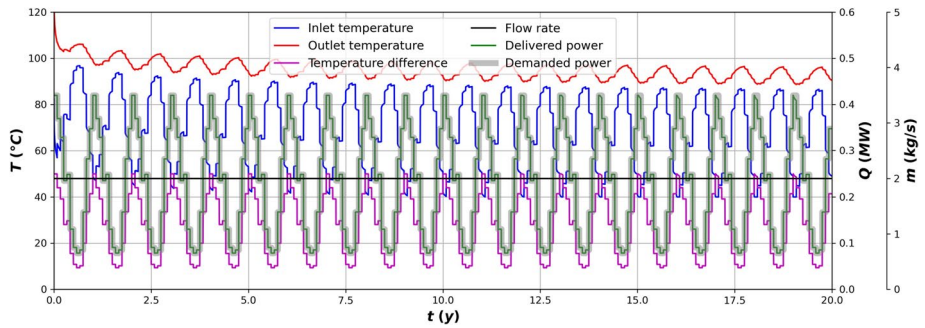

Fig. 12 Temperatures, flow rate, and gross thermal power delivered for Scenario 2 (irregular demand) with Control 1 (adjust of injection temperature) with constant flow rate ($m = 2$ kg/s)

Energy demand: scenario 2

Control 1: adjusting injection temperature

For Scenario 2 with Control 1, two relatively low and constant flow rates (2 and 3 kg/s) are chosen to try and ensure that the heat demand is always met. For the lower flow rate (Fig. 12), the necessary inlet temperature decreases with time and the minimum value

approaches the 40 °C threshold. The system covers the heat requirements for 12 years, but after that there is a power cut each year only at the end of the high demand periods, as the inlet temperature is about to drop below 40 °C. For the rest of the year the inlet temperature remains above 40 °C.

For the higher flow rate (3 kg/s) the heat demand is always met, as shown in Fig. 13a. Inlet and outlet temperatures are falling year after year, but the former remains always above the minimum threshold. For a constant flow rate and the same annually demand profile, the evolution of the temperature difference between outlet and inlet is the same every year. Each year, the minimum and the maximum temperature differences between inlet and outlet correspond to the minimum and maximum peaks of the demand, respectively. The minimum inlet and outlet temperatures appears at the same time step but at the end of the period of high demand (Fig. 13b), whereas the appearance of the maximum inlet temperature coincides with the end of the minimum demand period. The maximum outlet temperature, on the other hand, occurs with a delay, at the end of the next period. The frequency of appearance of the minimum and maximum values is the same each year as soon as the system approaches its thermal stabilization after the second to third year. An optimization of the system could be performed to define the minimum required flow rate for delivering the demanded power to minimize the power consumption for pumping the fluid.

A comparison of the performance of the two systems of Control 1 is shown in Table 6. As long as the system with the lower flow rate covers the demand, the COP remains higher due to the lower energy consumption for pumping. Even after the power cut at year 12, the system continuous to perform better, and it is only after year 17 that the COP of the system with the higher flow rate becomes higher. The system with the

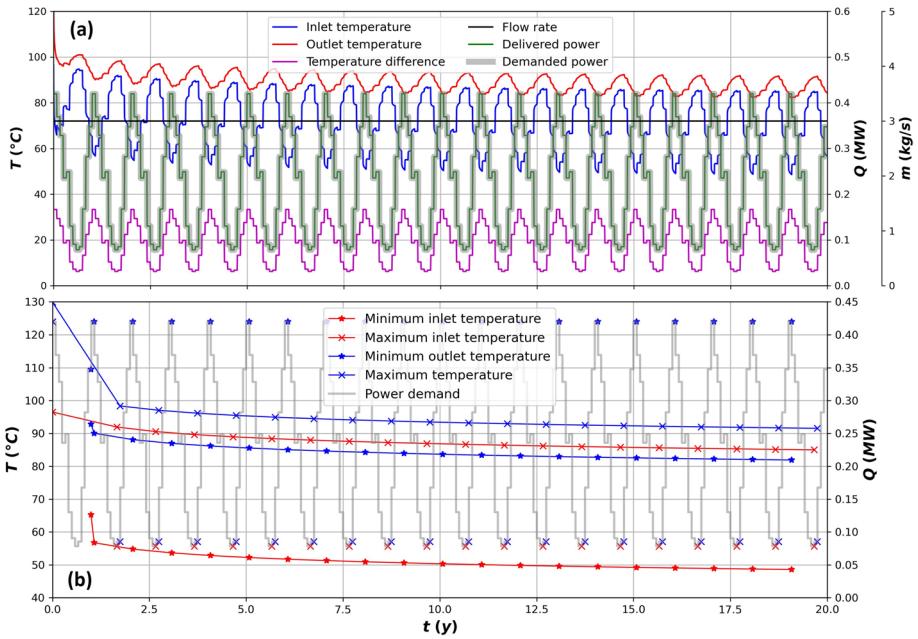

Fig. 13 **a** Temperatures, flow rate, and gross thermal power delivered, and **b** tracking of minimum and maximum inlet and outlet temperatures for Scenario 2 (irregular demand) with Control 1 (adjust of injection temperature) with constant flow rate ($m = 3$ kg/s)

Table 6 COPs for Control 1 (adjust of injection temperature) and Scenario 2 (irregular demand)

m_{init} (kg/s)	ΔP (bar)	T_{inj} (°C)	W_{pump} (MWh)	COP (cumulative)	COP (@ 1st year)	COP (@ 12th year)	COP (@ 17th year)	COP (@ 20th year)
2	1.7	>40	71	575	584	452	173	128
3	3.7	>48.6	229	177	177	177	177	177

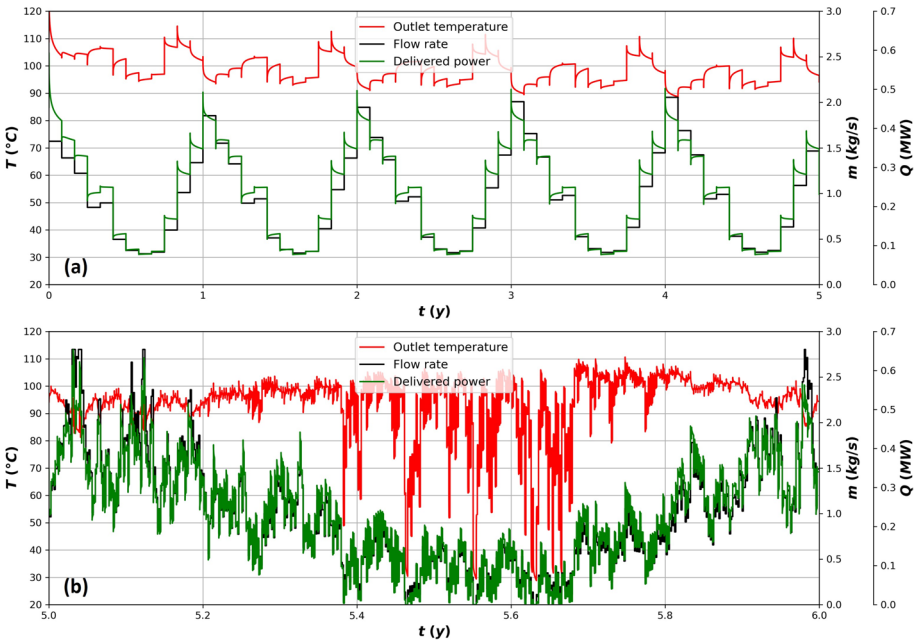

Fig. 14 Outlet temperature, required flow rate, and gross thermal power delivered for Scenario 2 (irregular demand) with Control 2 (adjust flow rate) for **a** monthly and **b** 12-h demand

lower flow rate covers 99.9%, 99.6% and 99.4% of the demand for years 12, 17 and 20, respectively.

Control 2: adjusting injection flow rate

For Scenario 2 and Control 2, first a total period of 6 years is simulated. During the first 5 years, 1-month timesteps are used and the system is meeting the monthly average heat demands. In the 6th year, the timestep is reduced to 12 h to capture the full 12-hourly peaking demands. This setup is designed to first deplete the heat in the rock over 5 years of consistent usage (heat requirements), then assess whether the well can meet the expected shorter-term peaks over the course of a year.

Figure 14 shows the evolution of the outlet temperature and flow rate for the previous mentioned conditions. Even the peak hourly demands are easily met during the last year. The required flow rate always follows the irregularities of the heat demand, with high power resulting in high flow rates. These flow rates experiment the highest changes when daily heat demand is considered. The output temperature during production is always over 75 °C, larger than the minimum required temperature of 45 °C, and only falls below when the required power/flow is zero. In the sixth year (12-h period), the temperature of the stagnant fluid is higher than that of the rocks and tends to reinitialize in

the initial temperature profile. This simulation shows that the well is likely overdesigned for the requirement at VITO facilities.

Over a period of 20 years, the minimum temperature remains still above 75 °C, whereas the required maximum flow rate is below 2.5 kg/s, as seen in Fig. 15. Only the first year, a steep decrease of the outlet temperature and increase of the flow rate is observed. After, the rate of evolution of the parameters decreases. The maximum flow rate, which increases each year, appears when the power demand is the maximum, whereas the minimum flow rate, which remains practically constant, corresponds to the minimum power.

Control 3: dual control system

For the dual control system and Scenario 2 a different approach is tested, in relation to Scenario 1, to avoid the consecutive adjustments of the flow rate once the temperature reaches the minimum threshold. A relatively low flow rate (1.5 kg/s) capable of covering the initial maximum peak is chosen as constant flow rate and, according to Control 1, the adjustment of the inlet temperature follows the power demand. Every time the inlet temperature is due to drop below the 40 °C limit, a step increase in the flow (by 1 kg/s) is triggered. The new flow rate is then kept constant, and the process follows the Control 1.

The evolution of the temperatures, flow rate and power are shown in Fig. 16a. The inlet temperature is due to fall below 40 °C during the maximum peak of the second year and for that reason the flow rate increases. The increase in the flow rate is accompanied by an increase of more than 20 °C compared with a system without control process (62 °C instead of less than 40 °C), which, however, is absorbed quite rapidly. Comparing the evolution of both temperatures with Control 1 (Fig. 13) it is obvious that the initial rate of decay is much faster for Control 3. The system with Control 3 compensates the lower

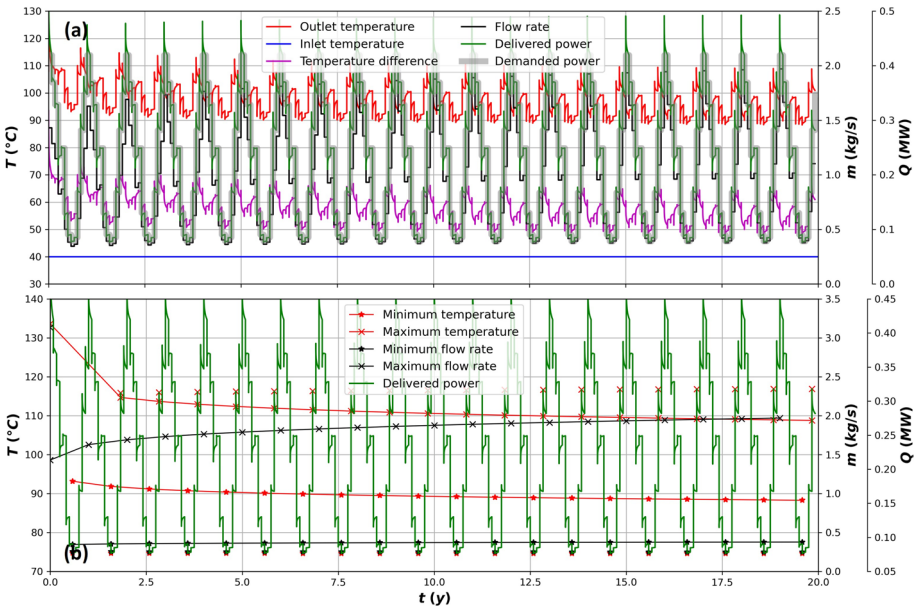

Fig. 15 **a** Temperature, flow rate, and gross thermal power delivered, and **b** tracking of minimum and maximum outlet temperature and flow rate for the Scenario 2 (irregular demand) with Control 2 (adjust flow rate) for 20 years of monthly demand

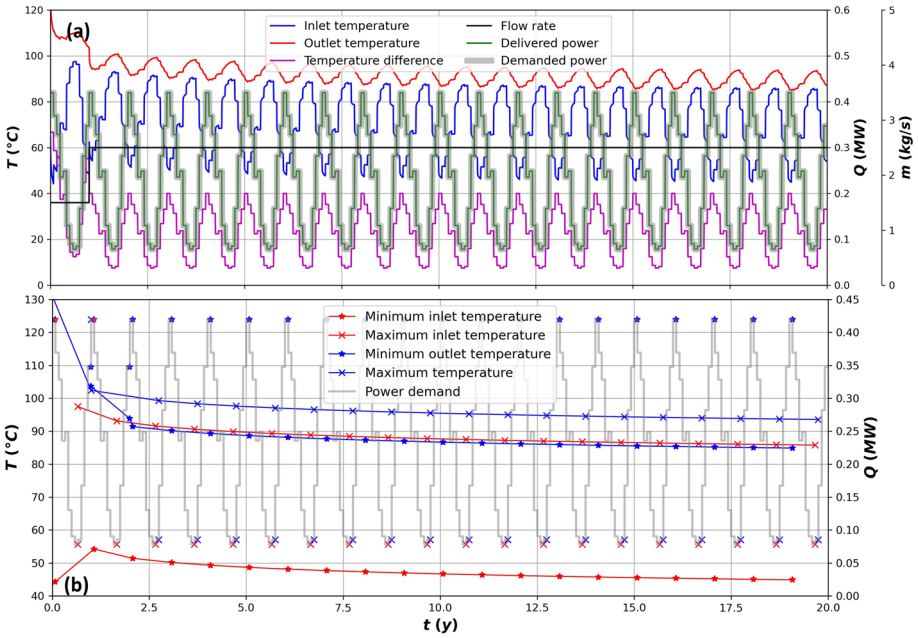

Fig. 16 **a** Temperatures, flow rate, and gross thermal power delivered, and **b** tracking of minimum and maximum inlet and outlet temperatures for Scenario 2 (irregular demand) with Control 3 (dual adjustment with $\Delta m = 1$ kg/s)

flow rate with larger temperature differences, thus lower inlet, and outlet temperatures. The minimum and maximum inlet and outlet temperatures occur at the same intervals as in Control 1 (Fig. 16b).

It should be noted that the behaviour of the system is highly dependent on the strategy chosen and the initial power demand. A detailed optimization procedure is required to define the initial and the progressive increase in the flow rate. On the other hand, starting the calculations from the months with the lowest power demand will result in a different evolution of the temperatures and the flow rate during the initial phases of the process. Nevertheless, the long-term response of the system should be the same whatever the initial conditions.

Figure 17 presents the results of a case with a lower step increase and Table 7 the comparison in the performance between the two systems of Control 3. The behaviour of the two systems is similar, and the final state of the fluid (flow rate and temperatures) is almost the same. The first increase in the flow rate occurs at exact the same moment since the initial flow rate is the same, but more steps are then needed for the lowest increment. For the lower step case, the performance improves because the flow rate remains lower for larger periods of time and the power consumption of the pump is smaller.

Discussion

Impact of inlet conditions

In the full-scale simulations for evaluating the potential of the site, the properties of the working fluid are pressure and temperature dependent. The results of Fig. 6 indicate that the average difference in the temperatures of the vertical water column

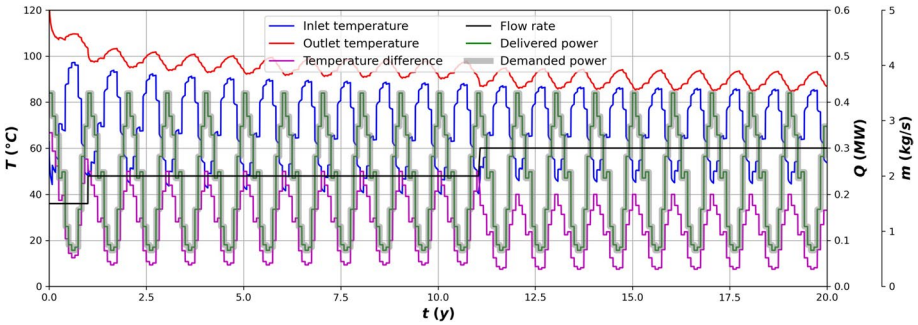

Fig. 17 Temperatures, flow rate, and gross thermal power delivered for Scenario 2 (irregular demand) with Control 3 (dual adjustment with $\Delta m = 0.5$ kg/s)

Table 7 COPs for Control 3 (dual adjustment) and Scenario 2 (irregular demand)

Δm (kg/s)	m_{max} (kg/s)	ΔP (bar)	T_{inj} (°C)	T_{prod} (°C)	W_{pump} (MWh)	COP (cumulative)	COP (@ 20th year)
0.5	2.5	< 2.6	< 62.7	> 86.7	96.7	308	420
1	2.5	< 2.6	< 64.5	> 87.1	130.2	299	312

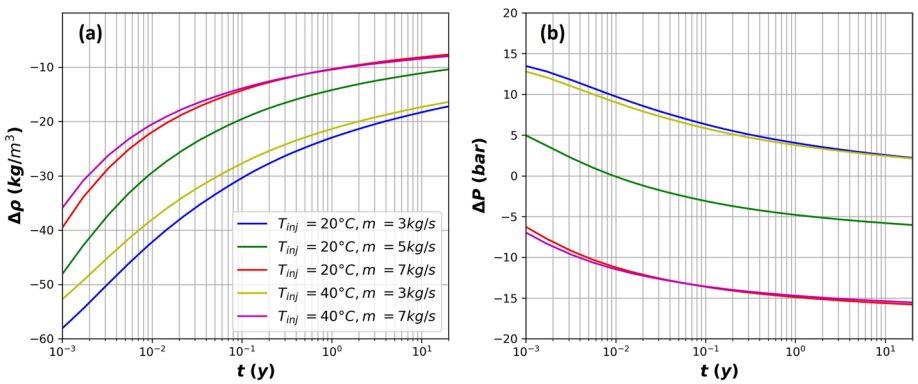

Fig. 18 Temporal evolution of a density and b pressure difference between well outlet and inlet

inside and outside of the well completion string is ranging between 30 and 50 °C. It is to note that this gives a difference in the density between 10 and 50 kg/m^3, for the 5000 m deep vertical well example and a flow rate of 5 kg/s (Fig. 18a). This density difference implies a pressure difference of the water column inside and outside the completion string in the order of few bars (Fig. 18b), leading to a self-propellant thermosiphon water flow circulation in the loop that could be sufficient (under certain conditions) to keep the circulation in the loop, with reduced or no need for external pumping power (Esmaeilpour et al. 2022). This phenomenon deteriorates with time due to the decreasing temperature differences in the vertical water columns and strongly depends on the inlet flow rate. For low flow rates, the outlet pressure is always higher than the inlet pressure, whereas for higher flow rates, the pressure difference may change sign or even be continuously negative. In addition, the pressure

gain must be sufficient to compensate any pressure losses in the surface installations to bypass the pump.

Impact of fluid properties

To support the choice of using constant fluid properties instead of pressure–temperature dependant properties a full-scale case is simulated with the two options. The results show that the impact on the outlet temperature (Fig. 19a) and gross thermal power output (Fig. 19b) is minor. With constant properties, the outlet temperature and thermal power are lower than 0.7–1.1% and 0.4–1.3%, respectively.

Thermal evolution of rock domain

Since the fluid retrieves thermal energy from the rocks, the temperature of the surrounding rock domain changes with time. The rate of change depends on the inlet conditions of the fluid and both the axial and the radial distance in the formation. Figure 20 depicts the evolution of the temperature difference in 3 depths and 4 radial distances for 2 flow rates. The temperature difference corresponds to the difference between the actual temperature and the initial temperature (the geothermal temperature at the specific depth). The rock temperature reduces with time, and the impact is stronger for higher flow rates, deeper in the formation and closer to the wellbore. As already mentioned, at higher flow rates more thermal heat is recovered from the hot rocks and as a result the temperature decreases faster. Deeper in the formation, the initial temperature difference between the fluid and the rocks is higher, thus the reduction is steeper and more pronounced. Similarly, the impact is stronger closer to the well, and in distance of around 50 m is practically negligible even after 20 years.

On the other hand, at higher inlet temperatures (Fig. 21), the fluid losses heat towards the rocks at a depth of several hundred of metres because the rocks are colder than the fluid. As a result, the rock temperature close to the surface increases (dashed blue line in Fig. 21). Deeper in the domain, the behaviour is similar to the previous case, with the difference that the decrease in rock temperature occurring more slowly due to the smaller temperature difference between the fluid and the rocks.

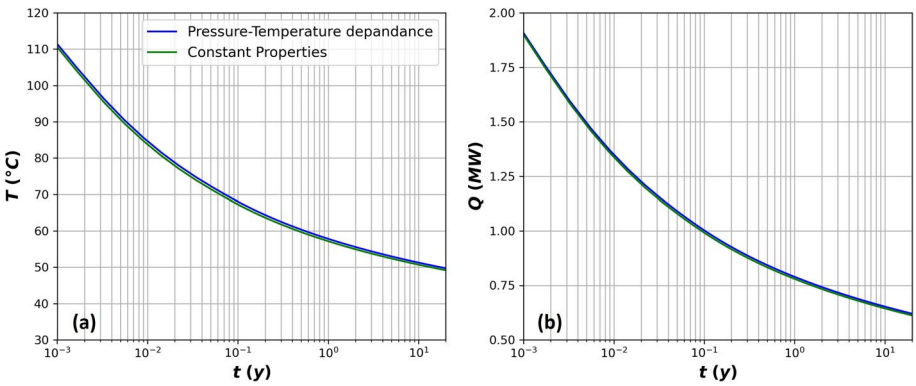

Fig. 19 Impact of water properties calculations on the a outlet temperature and b gross thermal power production ($m = 5$ kg/s, $T_{inj} = 20$ °C)

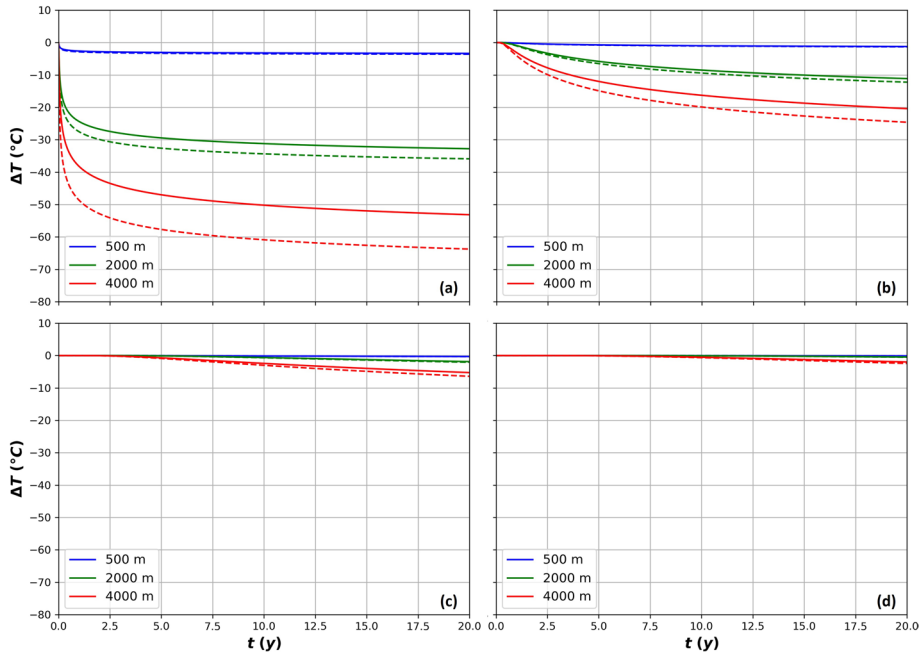

Fig. 20 Evolution of rock temperature in three depths and four radial distances: **a** 1 m, **b** 10 m, **c** 33 m and **d** 50 m for 3 kg/s (solid lines) or 7 kg/s (dashed lines) flow rate and 20 °C injection temperature

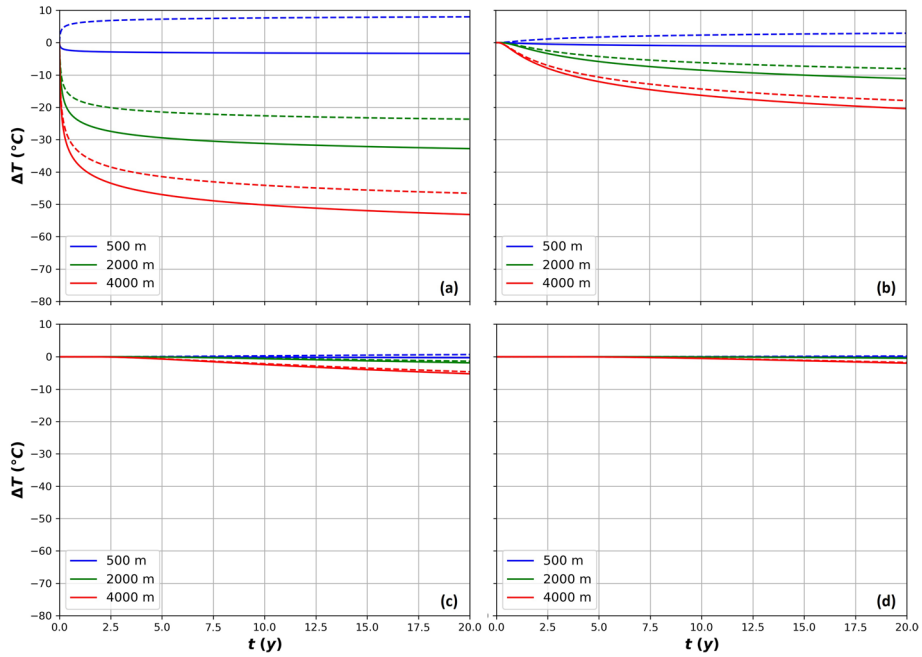

Fig. 21 Evolution of rock temperature in three depths and four radial distances: **a** 1 m, **b** 10 m, **c** 33 m and **d** 50 m with 20 °C (solid lines) or 40 °C (dashed lines) injection temperature and 3 kg/s flow rate

Scenario 1

In Fig. 22a, the cumulative COP of the optimal cases for Controls 1 and 3, and Control 2 are compared, whereas Table 8 summarizes the results for calculating the COP. The

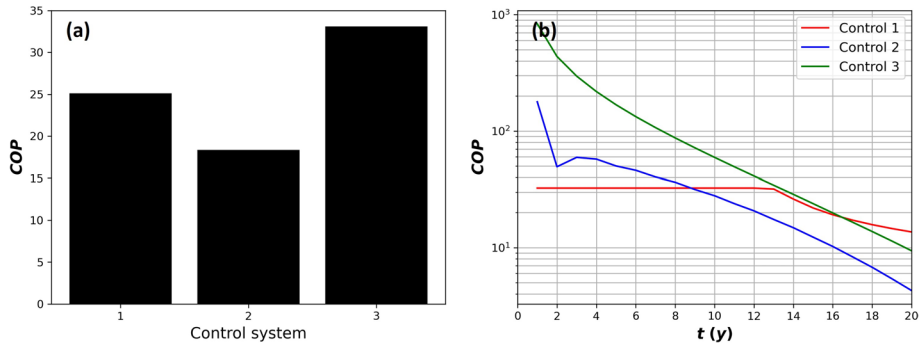

Fig. 22 Comparison of the a cumulative COP and b the yearly COP of all control systems for Scenario 1 (constant demand)

Table 8 COPs of all control systems and Scenario 1 (constant demand)

Control	m (kg/s)	ΔP (bar)	T_{inj} (°C)	T_{prod} (°C)	Q_{cov} (%)	W_{pump} (GWh)	COP (cumulative)	COP (@ 20th year)
1	7	18.7	< 97.5	> 56.3	99	2.69	25.5	13.6
2	< 14.2	< 75.5	40	> 48.4	100	4.66	18.4	4.3
3	< 11.0	< 45.0	< 72.4	> 50.8	100	3.41	33.1	9.4

freedom to choose the optimal injection flow rate in Control 1 allows that control to have a slightly better COP than in Control 2, which is constrained by the building to a fixed injection temperature. Thus, for covering the energy demand higher flow rates are needed over time which increase the pumping energy and decrease the cumulative COP. From an overall point of view, the best control strategy is the dual control as it provides the highest cumulative COP. This control takes advantage of both systems: it allows to keep low the expended pumping energy at early times by increasing the temperature difference while maintaining a low flow rate (Control 1). Furthermore, it can cover the energy demand in the long run by increasing the flow rate, which increases the well heat transfer coefficient and the temperature difference between the rock and the working fluid. Consequently, an increase of the heat flow at the cost of increasing expended pumping energy is achieved (Control 2).

From a punctual point of view, Control 2 and Control 3 may lead to high flow rates in the long-term resulting in non-permissible values of COP. In this case study, the COP at 20 years for Control 2 is 4.3, which is the lowest between the 3 studied controls (Table 8). This value could be still permissible but any further attempt to prolong the extraction at the same power will lead to values close or lower than 1 because the required flow rate and corresponding pressure drop will increase exponentially. The highest COP is for Control 1 with a value of 13.6. Control 3 shows a COP at the 20th year of 9.4 that can also decrease if the heating requirements are prolonged. With Control 1 and while the system is meeting the 0.5 MW, the annual COP remains constant, but lower than the COP of Control 2 and 3 (Fig. 22b). As soon as the flow rate of Control 2 and 3 exceeds the flow rate of Control 1 (7 kg/s in this case), the corresponding COPs are smaller.

Based on the overall and punctual analysis, Control 3 seems to be the best strategy to produce a constant power of 0.5 MW at temperature higher or equal than 45 °C, because

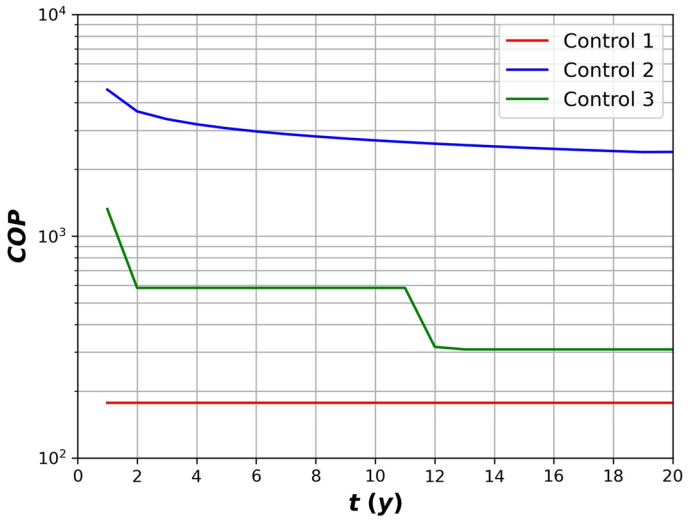

Fig. 23 Comparison of the yearly COP of all control systems for Scenario 2 (irregular demand)

Table 9 COPs of all control systems and Scenario 2 (irregular demand)

Control	m (kg/s)	ΔP (bar)	T_{inj} (°C)	T_{prod} (°C)	W_{pump} (MWh)	COP (cumulative)	COP (@ 20th year)
1	3	3.7	> 48.6	> 81.9	229	177	177
2	< 2.0	< 1.7	40	> 88.3	16	2542	2398
3	< 2.5	< 2.6	> 40.1	> 86.7	96.7	308	420

the cumulative COP is the highest and the COP at 20 years is not prohibited and can cover the whole demand.

Adjusting the flow rate (Control 2 or 3) requires a pumping system capable of delivering a flow over a wide range of flow rates, otherwise a power shortage is observed. Moreover, a secondary heat exchanger to deliver the fluid in the well at the desired temperature is required for all control systems. Both these observations need to be considered in the detailed design of the process.

Scenario 2

The annual COP of Control 1 is constant each year (Fig. 23), as the system is continuously covering the energy demands with a constant flow rate (the case with the higher flow rate is considered), whereas for the optimal Control 3, the COP decreases in the 2nd and the 11th years due to the increase in the flow rate to balance the forthcoming drop in the inlet temperature below the threshold. On the contrary, the COP for Control 2 decreases over time due to the gradual increase in the flow rate which is occurring to compensate for the decrease of the outlet temperature.

The higher COP of Control 2 is a result of the lower flow rates, resulting therefore to lower power consumption of the pump (Table 9). However, the performance of Controls 1 and 3 can be further improved by optimizing the imposed flow rate, as previously shown. It is obvious from the evolution of the inlet and outlet temperatures, which

remain above the minimum thresholds, that the selected flow rates for Control 1 and the step strategy for Control 3 are pessimistic and can be reduced. Lower flow rates mean lower energy consumption for pumping and a higher outlet temperature for the same power production, but a faster decline in performance because rocks temperature drops more quickly.

For the selected energy demand scenario, the operating range of the pump (for Controls 2 and 3) is limited compared to Scenario 1. However, the pump would have to continually adjust the flow rate (for Control 2) to meet the demand. One solution is to design the system to cover average monthly or seasonal periods of demand, so that the flow rates are set to respond to the daily peak demands within these periods by changing the injection temperature, such that the flow rate of the pump does not have to change continuously. In this case, and similarly to Scenario 1, a secondary heat exchanger is required to adjust the temperature of the injected fluid.

In case of higher peaks than those in Fig. 2, for example in case of extreme weather conditions, the geothermal system under consideration and with Control 2 (or 3) is expected to cover them. But higher flow rates are required with a corresponding increase in power consumption from the pump. On the other hand, the Control 1 would probably face a power lack because the minimum injection temperature has been set to 40 °C.

Conclusions

Two numerical tools are used in the study to simulate the potential reuse of an existing well in Mol, Belgium as a deep coaxial closed borehole heat exchanger by installing a central tubing in the current inclined well. Initially, the two codes are validated against an analytical solution for closed geothermal systems and compared to two commercial software. It is shown that both codes can predict the temporal evolution of the temperature in the well considering the heat transfer from a homogenous rock domain.

Full-scale simulations, considering the actual wellbore and geology, show that the site has a potential of delivering up to 2 MW of thermal energy at early times, depending, however, on the injection flow rate and temperature. For fixed inlet conditions, both the outlet temperature and the produced energy decrease over time, due to the highly transient nature of the diffusive heat transfer from the rocks to the wellbore, with the rate of decay being higher in the first few months of operation. After 20 years, the output energy is around 0.5 MW for all tested cases under different inlet conditions. The higher the flow rate and the lower the inlet temperature, the more total power is produced by the system. Thus, for the system to be able to supply specific heat, whether constant or irregular over time, the inlet conditions need to be adjusted accordingly. Moreover, the system can benefit from a reduction in pumping energy consumption due to the difference in fluid's density (thermosyphon effect) between the injection and the production sections, mainly for low flow rates and injection temperatures.

To define the injection conditions for meeting a constant heat demand profile (Scenario 1), three well controls are tested: Injection temperature optimization (Control 1),

injection flow rate optimization (Control 2) and a sequential use of the previous two controls (Control 3). Control 1 allows to keep a rather constant pumping energy consumption (since the injection flow rate is constant), but it struggles to fulfil the long-term demand profiles unless high flow rates are imposed which result in prohibited cumulative COP of the system (pump and underground heat exchanger). Control 2 allows a gradual increase of the injection flow rate overtime, improving the initial COP. Nevertheless, when the rocks are depleted, higher flow rates are needed to cover the demand, resulting in lower COP. The sequential use of Control 1 followed by Control 2 appears to be a better solution because the well can be started with a constant low flow rate at early times maximizing COP. When injection temperature reaches the minimum threshold, the flow rate is increased to enhance the heat flow rate with a corresponding decrease on the COP due to the higher needs in pumping power.

For highly irregular heat demands (Scenario 2), that are representative of actual buildings demands, largest changes in temperatures for Control 1 or continuous adjustments in flow rate are required in Control 2. A step increase of the flow rate every time the required inlet temperature is due to drop below 40°C is tested as Control 3 for Scenario 2. The system struggles to deliver the peak demand during the second year and the flow rate must be increased, which triggers a peak in the inlet temperature. Under the selected conditions, Control 2 seems to be the optimal control system for irregular demands due to the low flow rates. However, the exact injection methodology (initial flow rate and size of flow rate increment) needs to be optimized, also considering that the findings during the initial stages depend on the profile of the imposed heat demand.

The implementation of the control strategies will impact the design and operation of the full system. On the one hand, adapting the flow rate would require a pumping system capable of delivering a flow over a wide range of flow rates, otherwise there could be a power shortage. On the other hand, a secondary heat exchanger would be required in the surface to deliver the injection fluid at constant temperature. Finally, adapting the injection temperature would also require the use of a secondary heat exchanger together with a pump for injecting the fluid. In this work the secondary heat exchanger is not considered. Simulations of the underground closed-loop and the above-ground energy system is a work in progress as part of the HOCLOOP project to define the optimum wellbore configuration and operational conditions, considering the control systems and any potential pressure gain that may be caused by the thermosiphon effects.

Appendix

In the below tables the necessary data to reproduce the results are provided for the case study and the benchmarking simulations.

See Tables 10, 11, 12, 13

Table 10 Description of thermal rock properties, temperature gradient and temperature along the well

Thermal rock layers	Bottom trajectory [m MD]	Bottom depth [m TVD]	k [W/m/°C]	Cp [J/kg/K]	ρ [kg/m^3]	g_T [°C/m TVD]	Temperature at layer bottom [°C]
Surface	0	0					11
Cenozoic	636	635.8	2.00	930	2360	0.029	29
Cretaceous–Mesozoic	897.5	897.1	1.89	800	2360	0.029	37
Upper carboniferous–Paleozoic	3643	3141.6	1.36	903.5	2530	0.043	134
Lower carboniferous–Paleozoic	4747	4082	2.70	933.8	2700	0.021	153
Devonian–Paleozoic	4905	4230	2.48	933.8	2700	0.021	156

Table 11 Dimensions and thermal properties of the casings and cement tubulars in well MOL-GT-03

Well layer ID	Top trajectory depth [m]	Bottom trajectory depth [m]	OD [inches]	ID [inches]	Type
1	0	30	32	31.5	Conductor
2	0	206	24	23.5	Casing
3	0	874	18.625	17.755	Casing
4	0	2183	13.375	12.347	Casing
5	2067	3600	9.625	8.535	Liner
6	3533.2	3750	7	6.184	Liner
7	3750	4905	8.5		Open-Hole
8	0	206	31.5	24	Cement
9	0	874	23.5	18.625	Cement
10	0	2183	17.755	13.375	Cement
11	2067	3600	12.5	9.625	Cement

Casing: $k = 45$ W/m/K, $Cp = 420$ J/kg/K, $\rho = 7000$ kg/m^3

Cement: $k = 0.896$ W/m/K, $Cp = 1400$ J/kg/K, $\rho = 3140$ kg/m^3

Table 12 Characteristics of the insulated tubing

ID [mm]	ε [mm]	k [W/m/K]	Cp [J/kg/K]	ρ [kg/m^3]
42.5	27.5	0.0264	500	300

Table 13 Data of benchmarking case

Well	Direction	Vertical
	Type	Closed
	Depth, H (m)	1828.2
Tubing	Inner diameter, d_{ti} [m]	0.05
	Outer diameter, d_{to} [m]	0.08
	Conductivity, k_t [W/m/K]	0.1
Casing	Inner diameter, d_{ci} [m]	0.1617
	Outer diameter, d_{co} [m]	0.1778
	Conductivity, k_c [W/m/K]	43.268
Temperatures	Surface, T_{surf} [°C]	21.111
	Gradient, g_T [°C/m]	0.01513
	Injection, T_{inj} [°C]	14.72
Rocks	Conductivity, k_e [W/m/K]	2.423
	Density, ρ_e [kg/m^3]	2600
	Heat capacity, C_{pe} [J/kg/K]	902.67
Fluid	Flow rate, m [kg/s]	8.8
	Density, ρ_f [kg/m^3]	998.554
	Viscosity, μ_f [mPa.s]	1.1
	Thermal conductivity, k_f [W/m/K]	0.5867
	Heat capacity, Cp_f [J/kg/K]	4196

List of symbols

Symbols

Cp	Heat capacity [J/kg/K]
D	Depth [m]
d	Diameter [m]
E	Total produced power or energy [Ws or GWh]
H	Total measured depth of the computational domain [m]
g_T	Geothermal gradient [°C/m]
k	Thermal conductivity [W/m/K]
L	Total measured length of the wellbore [m]
m	Mass flow rate [kg/s]
P	Pressure [bar]
Q	Power or energy [W]
r	Radial coordinate
R	Total radius of the domain [m]
t	Time [s]
T	Temperature [°C]
z	Vertical coordinate
Z	Axial coordinate (along the inclined wellbore)

Greek symbols

Δ	Difference
ε	Thickness [m]
θ	Wellbore inclination [°]
ρ	Density [kg/m^3]

Subscripts

c	Casing
f	Fluid
e	Rocks/formation
i	Row number of the axial grid
init	Initial
inj	Injection or inlet
j	Column number of the radial grid
out	Outlet or production
prod	Produced
ref	Reference or demanded

res	Reservoir
surf	Surface
t	Tubing

Abbreviations

COP	Coefficient of performance
DBHE	Deep borehole heat exchanger
EoS	Equation of state
ID	Inner diameter
MD	Measured depth
OD	Outer diameter
TVD	True vertical depth

Acknowledgements
This work was supported by the European Union's Horizon Research and Innovation Program through Agreement no. 101083558 (the HOCLOOP Project). The authors would like to acknowledge Reelwell A.S., industrial partner of the HOCLOOP project, and Ola Vestavik, CEO of Geothermal and HOCLOOP partner, for providing details and technical data of the potential well completion string. Also, Hung Pham from Technical University of Darmstadt, HOCLOOP partner, for providing the results of the numerical simulations with FEFLOW.

Author contributions
VL: conception, design of the work, creation of software (GWellFM), acquisition and interpretation of data (GWellFM), drafted the work; EH: conception, design of the work, acquisition and interpretation of data (COMSOL), drafted the work; JP: acquisition and interpretation of data (GWT), drafted the work; MW: creation of software (GWT), interpretation of data (GWT); VH-M: revision.

Funding
The present research was funded by the European Union's Horizon Research and Innovation Program under grant agreement No. 101083558 (HOCLOOP Project).

Availability of data and materials
No datasets were generated or analysed during the current study.

Declarations

Ethics and consent to participate
Not applicable.

Competing interests
The authors declare no competing interests.

Received: 18 October 2024 Accepted: 3 January 2025
Published online: 30 January 2025

References

Abesser C, Schincariol RA, Raymond J, García-Gil A, Drysdale R, Piatek A, Giordano N, Jaziri N, Molson J. Case studies of geothermal system response to perturbations in groundwater flow and thermal regimes. Ground Water. 2023;61:255–73. https://doi.org/10.1111/gwat.13086.

Al Saedi AQ, Flori RE, Kabir CS. New analytical solutions of wellbore fluid temperature profiles during drilling, circulating, and cementing operations. J Petrol Sci Eng. 2018;170:206–17. https://doi.org/10.1016/j.petrol.2018.06.027.

Alimonti C, Soldo E, Bocchetti D, Berardi D. The wellbore heat exchangers: a technical review. Renew Energy. 2018;123:353–81. https://doi.org/10.1016/j.renene.2018.02.055.

Amaya A, Scherer J, Muir J, Patel M, Higgins B. GreenFire energy closed-loop geothermal demonstration using supercritical carbon dioxide as working fluid. In: Proceedings of the 45th Workshop on geothermal reservoir engineering; Stanford 10–12/02: SGP-TR-216. 2020.

Beckers KF, Rangel-Jurado N, Chandrasekar H, Hawkins AJ, Fulton PM, Tester JW. Techno-economic performance of closed-loop geothermal systems for heat production and electricity generation. Geothermics. 2022;100:102318. https://doi.org/10.1016/j.geothermics.2021.102318.

Bos S, Ben L. Development of the first deep geothermal doublet in the Campine Basin of Belgium. European Geol J. 2017;43:16–20.

Buijze L, van Bijsterveldt L, Cremer H, Paap B, Veldkamp H, Wassing BB, van Wees J-D, van Yperen GC, ter Heege JH, Jaarsma B. Review of induced seismicity in geothermal systems worldwide and implications for geothermal systems in the Netherlands. Neth J Geosci. 2019. https://doi.org/10.1017/njg.2019.6.

Chen H, Tomac I. Technical review on coaxial deep borehole heat exchanger. Geomech Geophys Geo-energ Geo-resour. 2023. https://doi.org/10.1007/s40948-023-00659-4.

Chen J, Huang W, Cen J, Cao W, Li Z, Li F, Jiang F. Heat extraction from hot dry rock by super-long gravity heat pipe: selection of working fluid. Energy. 2022;255:124531. https://doi.org/10.1016/j.energy.2022.124531.

Chen J, Li Z, Huang W, Ma Q, Li A, Wang B, Sun H, Jiang F. Super-long gravity heat pipe geothermal space heating system: a practical case in Taiyuan, China. Energy. 2024;299:131521. https://doi.org/10.1016/j.energy.2024.131521.
Daniilidis A, Nick HM, Bruhn DF. Interference between geothermal doublets across a fault under subsurface uncertainty; implications for field development and regulation. Geothermics. 2021;91:102041. https://doi.org/10.1016/j.geothermics.2021.102041.
de Hemptinne J-C, Ferrando N, Hajiw-Riberaud M, Lachet V, Maghsoodloo S, Mougin P, Ngo TD, Pigeon L, Romero Yanes J, Wender A. Carnot : a thermodynamic library for energy industries. Sci Tech Energ Transition. 2023;78:30. https://doi.org/10.2516/stet/2023023.
de Rose A, Harcouët-Menou V, Laenen B, Caia V, Facco L, Guglielmetti L, et al. Study on 'geothermal plants' and applications' emissions. In: de Rose A, Harcouët-Menou V, Laenen B, Caia V, Facco L, Guglielmetti L, editors., et al., Overview and analysis final report. Luxembourg: Publications Office of the European Union; 2020.
Dijkshoorn L, Speer S, Pechnig R. Measurements and design calculations for a deep coaxial borehole heat exchanger in Aachen, Germany. Geophys J Int. 2013;2013:1–14. https://doi.org/10.1155/2013/916541.
Esmaeilpour M, Gholami Korzani M, Kohl T. Impact of thermosiphoning on long-term behavior of closed-loop deep geothermal systems for sustainable energy exploitation. Renew Energy. 2022;194:1247–60. https://doi.org/10.1016/j.renene.2022.06.014.
Gascuel V, Rivard C, Raymond J. Deep geothermal doublets versus deep borehole heat exchangers: a comparative study for cold sedimentary basins. Appl Energy. 2024;361:122826. https://doi.org/10.1016/j.apenergy.2024.122826.
Guo Z, Dai Y, Zhang J, Gui X, He Y. Improved modeling analysis on heat transfer performance of deep coaxial borehole heat exchanger with different operation modes. Energy Rep. 2024;11:355–68. https://doi.org/10.1016/j.egyr.2023.11.066.
Hernandez Acevedo E, Rodriguez Hernandez I. A geothermal doublet in a single well: application of the recirculation well concept to reuse wells to be abandoned. Discov Energy. 2024. https://doi.org/10.1007/s43937-024-00048-2.
Hu X, Banks J, Wu L, Liu WV. Numerical modeling of a coaxial borehole heat exchanger to exploit geothermal energy from abandoned petroleum wells in Hinton, Alberta. Renew Energy. 2020;148:1110–23. https://doi.org/10.1016/j.renene.2019.09.141.
Hu Z, Xu T, Feng B, Yuan Y, Li F, Feng G, Jiang Z. Thermal and fluid processes in a closed-loop geothermal system using CO2 as a working fluid. Renew Energy. 2020;154:351–67. https://doi.org/10.1016/j.renene.2020.02.096.
Huajun W, Yishuo X, Yukun S, Sumin Z. Heat extraction by deep coaxial borehole heat exchanger for clean space heating near Beijing, China: field test, model comparison and operation pattern evaluation. Renew Energy. 2022;199:803–15. https://doi.org/10.1016/j.renene.2022.09.017.
Huchtemann K, Müller D. Combined simulation of a deep ground source heat exchanger and an office building. Build Environ. 2014;73:97–105. https://doi.org/10.1016/j.buildenv.2013.12.003.
Kohl T, Brenni R, Eugster W. System performance of a deep borehole heat exchanger. Geothermics. 2002;31:687–708. https://doi.org/10.1016/S0375-6505(02)00031-7.
Kolo I, Brown CS, Nibbs W, Cai W, Falcone G, Nagel T, Chen C. A comprehensive review of deep borehole heat exchangers (DBHEs): subsurface modelling studies and applications. Geotherm Energy. 2024. https://doi.org/10.1186/s40517-024-00297-3.
Kruszewski M, Montegrossi G, Saenger EH. The risk of fluid-injection-induced fault reactivation in carbonate reservoirs: an investigation of a geothermal system in the Ruhr region (Germany). Geomech Geophys Geo-energ Geo-resour. 2023. https://doi.org/10.1007/s40948-023-00573-9.
Le Lous M, Larroque F, Dupuy A, Moignard A. Thermal performance of a deep borehole heat exchanger: insights from a synthetic coupled heat and flow model. Geothermics. 2015;57:157–72. https://doi.org/10.1016/j.geothermics.2015.06.014.
Leontidis V, Niknam PH, Durgut I, Talluri L, Manfrida G, Fiaschi D, Akin S, Gainville M. Modelling reinjection of two-phase non-condensable gases and water in geothermal wells. Appl Therm Eng. 2023;223:120018. https://doi.org/10.1016/j.applthermaleng.2023.120018.
Lopez S, Hamm V, Le Brun M, Schaper L, Boissier F, Cotiche C, Giuglaris E. 40 years of Dogger aquifer management in Ile-de-France, Paris Basin, France. Geothermics. 2010;39:339–56. https://doi.org/10.1016/j.geothermics.2010.09.005.
Lund AE. Effect of heat and mass transfer related parameters on the performance of deep borehole heat exchangers. Appl Therm Eng. 2024;253:123764. https://doi.org/10.1016/j.applthermaleng.2024.123764.
Luo W, Kottsova A, Vardon PJ, Dieudonné AC, Brehme M. Mechanisms causing injectivity decline and enhancement in geothermal projects. Renew Sustain Energy Rev. 2023;185:113623. https://doi.org/10.1016/j.rser.2023.113623.
Manzella A, Serra D, Cesari G, Bargiacchi E, Cei M, Cerutti P, Conti P, Giudetti G, Lupi M, Vaccaro M. Geothermal energy use, country update for Italy. The Hague: European Geothermal Congress; 2019.
Melikoglu M. Geothermal energy in Turkey and around the World: a review of the literature and an analysis based on Turkey's Vision 2023 energy targets. Renew Sustain Energy Rev. 2017;76:485–92. https://doi.org/10.1016/j.rser.2017.03.082.
Morita K, Bollmeier WS, Mizogami H. An experiment to prove the concept of the downhole coaxial heat exchanger (DCHE) in Hawaii. Geotherm Resour Counc Trans. 1992;16:9–16.
Ragnarsson Á, Steingrímsson B, Thorhallsson S. Geothermal development in Iceland 2015–2019. Reykjavik: World Geothermal Congress; 2021.
Ramey HJ. Wellbore heat transmission. J Pet Technol. 1962;14:427–35. https://doi.org/10.2118/96-PA.
Santos L, Dahi Taleghani A, Elsworth D. Repurposing abandoned wells for geothermal energy: current status and future prospects. Renew Energy. 2022;194:1288–302. https://doi.org/10.1016/j.renene.2022.05.138.
Song X, Wang G, Shi Y, Li R, Xu Z, Zheng R, Wang Y, Li J. Numerical analysis of heat extraction performance of a deep coaxial borehole heat exchanger geothermal system. Energy. 2018;164:1298–310. https://doi.org/10.1016/j.energy.2018.08.056.
Vestavik OM, Thorogood J, Bourdelet E, Schmalhorst B, Roed JP. Horizontal drilling with dual channel drill pipe. In: Vestavik OM, Thorogood J, Bourdelet E, Schmalhorst B, Roed JP, editors. SPE/IADC drilling conference and exhibition. Hague: SPE/IADC; 2017. https://doi.org/10.2118/184683-MS.

Wang G, Song X, Shi Y, Yang R, Yulong F, Zheng R, Li J. Heat extraction analysis of a novel multilateral-well coaxial closed-loop geothermal system. Renew Energy. 2021;163:974–86. https://doi.org/10.1016/j.renene.2020.08.121.
Wang Y, Wang Y, You S, Zheng X, Cong P, Shi J, Li B, Wang L, Wei S. Mathematical modeling and periodical heat extraction analysis of deep coaxial borehole heat exchanger for space heating. Energy Build. 2022;265:112102. https://doi.org/10.1016/j.enbuild.2022.112102.
Wangen M. A semi-analytical temperature solution for multi-segment deep coaxial borehole heat exchangers. Geomech Geophys Geo-energ Geo-resour. 2024. https://doi.org/10.1007/s40948-023-00721-1.
Willems CM, Nick H. Towards optimisation of geothermal heat recovery: an example from the West Netherlands Basin. Appl Energy. 2019;247:582–93. https://doi.org/10.1016/j.apenergy.2019.04.083.

Publisher's Note